mL each) were stirred at a constant speed (ca. 250 rpm). Further details of the transport method were described previously.[6] The rates of ion transport were estimated by meausring the concentration of alkali metal cations transported to the OUT aqueous phase by atomic absorption spectroscopy (Shimadzu AA-640). One transport experiment was continued at least for 20 h, and the ion flux (J, mol s^{-1} cm^{-2}) was determined from the linear slope of the [M^+] vs. time plot. The permeability coefficients (P_{M^+}, s^{-1} cm^2) were calculated from eq 3, where l is the membrane thickness and C_{IN} and C_{OUT} are the metal concentrations in the IN and the OUT aqueous phase, respectively.

$$P_{M^+} = Jl/(C_{IN} - C_{OUT}) \quad (3)$$

Acknowledgment. This research was partly supported by the Grant-in-Aid on Special Project Research from the Ministry of Education, Science and Culture.

[1-^{13}C]Aldono-1,4-lactones: Conformational Studies Based on ^{1}H–^{1}H, ^{13}C–^{1}H, and ^{13}C–^{13}C Spin Couplings and ab Initio Molecular Orbital Calculations

Timothy Angelotti, Michael Krisko, Thomas O'Connor, and Anthony S. Serianni*

Contribution from the Department of Chemistry, University of Notre Dame, Notre Dame, Indiana 46556. *Received July 3, 1986*

Abstract: Several aldono-1,4-lactones have been synthesized with [^{13}C] enrichment (99 atom %) at the carbonyl carbon. ^{1}H (300 and 600 MHz) and ^{13}C (75 MHz) NMR spectra in ^2H_2O have been assigned, the latter with the aid of 2D ^{13}C–^{1}H chemical shift correlation spectroscopy. ^{1}H–^{1}H, ^{13}C–^{1}H, and ^{13}C–^{13}C couplings have been used to evaluate lactone ring conformations. In general, aldono-1,4-lactones in aqueous solution prefer conformations in which O2 is oriented quasi-equatorial. On the basis of ab initio STO-3G MO calculations of two representative lactones, it appears that this preference is not due to stabilization conferred by intramolecular hydrogen bonding, as generally believed, but to stereoelectronic factors found in α-hydroxy-γ-lactones. Theoretical calculations have also revealed a notable effect of lone-pair oxygen orbitals on C–H bond lengths, namely, that C–H bonds are longest when antiperiplanar to a lone-pair orbital. This dependence may be responsible, in part, for the observed ^{1}H chemical shift patterns for these molecules. A model has been proposed to rationalize the dependence of dual-pathway ^{13}C–^{13}C couplings on lactone ring configuration.

The conformational characteristics of five-membered rings have been the subject of scientific scrutiny for decades.[1] This interest has been stimulated in recent years because of the potential role that furanose ring conformation and dynamics play in the structure and function of nucleic acids in biological systems.[2] The simplest saturated five-membered ring, cyclopentane, exists in puckered (envelope, twist) conformations in solution[1d,e] in which the destabilizing effects of eclipsed C–H bonds are minimized. As either endocyclic or exocyclic heteroatoms are substituted/appended in the ring, additional molecular forces compete to determine preferred geometry.[3] Twenty puckered conformers can be assumed by dissymmetric furanose rings (10 envelope, 10 twist), and their spontaneous interconversion occurs by pseudorotation.[1a,4] In general, these conformers have similar energies. Conformational averaging, therefore, complicates the interpretation of the physical constants (e.g., NMR parameters)[5] of these structures.

We have shown that conformational analysis of furanose rings by NMR spectroscopy is notably improved by measuring ^{13}C–^{1}H and ^{13}C–^{13}C in addition to ^{1}H–^{1}H spin couplings in these rings.[3] Perlin and co-workers[6] have made similar arguments, namely, that "redundant" coupling measurements often improve the discrimination between conformers.

Replacement of a furanose ring sp^3 carbon by an sp^2 carbon (e.g., conversion to an aldono-1,4-lactone) causes considerable changes in ring conformation and dynamics. The planarity (or near-planarity) of the OC(O)C fragment restricts 1,4-lactone rings to two relatively small segments of the pseudorotational itinerary.[4] Because 1,4-lactone rings are important components of many natural products (e.g., antibiotics), we have examined the structural properties of several [1-^{13}C]aldono-1,4-lactones in aqueous (^2H_2O) solution by ^{1}H and ^{13}C NMR spectroscopy. ^{1}H and ^{13}C chemical shifts have been assigned, and ^{1}H–^{1}H, ^{13}C–^{1}H, and ^{13}C–^{13}C coupling constants have been measured and related

Table I. Preparation and Purification of D-[1-^{13}C]Aldonates

compound	method[a]	chromatography[b]
erythro **1**	A	0.5 M
threo **5**	A	0.5 M
arabino **6**, ribo **2**	B	0.35 M (2 L), then 0.5 M (3 L): ribo
lyxo **12**, xylo **9**	B	0.4 M (4 L): xylo
allo **3**, altro **7**	B	0.4 M (4 L): allo
galacto **8**, talo **4**	B	0.1–0.4 M LG[c] (4 L), followed by 0.4 M (2 L): talo
gluco **10**, manno **13**	B	0.7 M (3 L): gluco

[a] Method A: hypoiodite oxidation of the corresponding D-[1-^{13}C]-aldose. Method B: cyanohydrin synthesis. [b] Dowex 1 × 8 (200–400 mesh) in the acetate form; column size = 2.5 × 60 cm. Acetic acid was employed as the eluent using the concentrations and volumes indicated. Columns were eluted at a flow rate of ~1 mL/min (15-mL fractions), and fractions were assayed for aldonate with chromotropic acid.[13] The epimer that elutes first is identified. [c] LG = linear gradient.

(1) (a) Kilpatrick, J.; Pitzer, K.; Spitzer, K. *J. Am. Chem. Soc.* **1947**, *69*, 2485. (b) Altona, C.; Sundaralingam, M. *Ibid.* **1972**, *94*, 8205. (c) Gerlt, J. A.; Youngblood, A. V. *Ibid.* **1980**, *102*, 7433. (d) Poupko, R.; Luz, Z.; Zimmermann, H. *Ibid.* **1982**, *104*, 5307. (e) Cremer, D.; Pople, J. A. *Ibid.* **1975**, *97*, 1358.

(2) (a) de Leeuw, H. P. M.; Haasnoot, C. A. G.; Altona, C. *Isr. J. Chem.* **1980**, *20*, 108. (b) Levitt, M.; Warshel, A. *J. Am. Chem. Soc.* **1978**, *100*, 2607. (c) Olson, W. K.; Sussman, J. L. *Ibid.* **1982**, *104*, 270. (d) Olson, W. K. *Ibid.* **1982**, *104*, 278. (e) Westhof, E.; Sundaralingam, M. *Ibid.* **1983**, *105*, 970.

(3) Serianni, A. S.; Barker, R. *J. Org. Chem.* **1984**, *49*, 3292.

(4) Altona, C.; Sundaralingam, M. *J. Am. Chem. Soc.* **1972**, *94*, 8205.

(5) Jardetsky, O. *Biochem. Biophys. Acta* **1980**, *621*, 227.

(6) Cyr, N.; Perlin, A. S. *Can. J. Chem.* **1979**, *57*, 2504.

0002-7863/87/1509-4464$01.50/0

to ring configuration and conformation. Preferred solution conformations deduced from NMR data are compared with those predicted for "gas-phase" structures by ab initio molecular orbital calculations as a means to determine the factors responsible for stabilizing particular molecular geometries.

Experimental Section

A. Chemicals and Reagents. DL-Glyceraldehyde, D-arabinose, D-lyxose, D-ribose, D-xylose, D-ribono-1,4-lactone, D-galactono-1,4-lactone, D-gulono-1,4-lactone, and Dowex ion-exchange resins were obtained from Sigma Chemical Co. D-Erythrose[7] and D-threose[8] were prepared from 4,6-O-ethylidene-D-glucose and 4,6-*O*-ethylidene-D-galactose, respectively. Potassium [^{13}C]cyanide (K[^{13}C]N, 99 atom % ^{13}C) and deuterium oxide (^2H_2O, 98 atom % ^{2}H) were purchased from Cambridge Isotope Laboratories. Chromotropic acid (4,5-dihydroxynaphthalene-2,7-disulfonic acid, disodium salt dihydrate) was purchased from Aldrich Chemical Co.

B. Instrumentation. ^{1}H (300 MHz) and ^{13}C (75 MHz) NMR spectra were obtained at ambient temperature (~25 °C) on a Nicolet NT-300 FT-NMR spectrometer equipped with quadrature-phase detection and a 293B pulse programmer. The 600-MHz rapid-scan cross-correlated ^{1}H NMR spectra in ^2H_2O were obtained at the NMR Facility for Biomedical Studies, Department of Chemistry, Carnegie-Mellon University, Pittsburgh, Pa., which is partly supported by NIH Grant P41RR00292-19.

The observation of small couplings in ^{1}H and ^{13}C spectra was improved by multiplying FIDs by a double-exponential function (resolution-enhancement) prior to Fourier transformation. Lactone concentrations were ~0.1 M for ^{1}H and ~0.3 M for ^{13}C measurements in total solution volumes of 0.5 and 2.0 mL of ^2H_2O, respectively.

Two-dimensional ^{13}C–^{1}H chemical shift correlated spectra[9] were obtained on the Nicolet NT-300 spectrometer using software supplied by GE NMR Systems.

C. Preparations. [1-^{13}C]Aldono-1,4-lactones were prepared by the cyanohydrin (Kiliani) synthesis[10,11] or hypoiodite oxidation[12] (Table I).

Cyanohydrin (Kiliani) Synthesis.[10,11] The parent sugar (10 mmol) (Table I) was dissolved in 20 mL of distilled water at 4 °C, and K^{13}CN (10 mmol in 10 mL of distilled water at 4°) was added. The alkaline solution was stored at 4° overnight, and then kept at room temperature for 3–4 days. The solution was maintained at pH 10–12 over this time period, and the mixture of C2-epimeric [1-^{13}C]aldonates was chromatographed on a column (2.5 × 60 cm) of Dowex 1 × 8 (200–400 mesh) (OAc^-) using dilute acetic acid as the eluent (Table I).[11] Fractions were assayed for aldonate with chromotropic acid,[13] and those containing labeled aldonate were pooled and the solution was concentrated in vacuo at 30 °C to a syrup.

To achieve lactonization, syrups were dissolved in a minimum amount of water and the solutions passed through columns containing >10-fold excess of Dowex 50 × 8 (200–400 mesh) (H^+) using deionized water as the eluent. These deionized solutions were concentrated to syrups at 30 °C in vacuo and the syrups stored in a desiccator under vacuum with $MgClO_4$ for at least 4 days.

Hypoiodite Oxidation. D-[1-^{13}C]Erythronate and D-[1-^{13}C]threonate were obtained by hypoiodite oxidation[12] of D-[1-^{13}C]erythrose and D-[1-^{13}C]threose, prepared and purified as described previously.[14,15] The labeled aldonates were purified from reaction by-products by Dowex 1 chromatography and lactonized according to procedures described above.

D. Molecular Orbital Calculations on Erythrono-1,4-lactone (1) and Threono-1,4-lactone (5). Ab initio molecular orbital calculations were conducted at the STO-3G[16a] level using Gaussian 80[16b] as implemented on an IBM 370/3033 mainframe computer (Notre Dame Computing Center). Four envelope forms (E_3, ^3E, E_4, ^4E) and the planar conformation (P) of **1** and **5** were considered. All molecular parameters (bond lengths, angles, and torsions) were optimized by analytic gradient methods, with the exception of the 0° endocyclic torsion angle(s) required to constrain the calculation to an envelope or planar conformer. Approximately 5 h of CPU time per conformer was required to achieve convergence (see Appendix for details).

Chart I

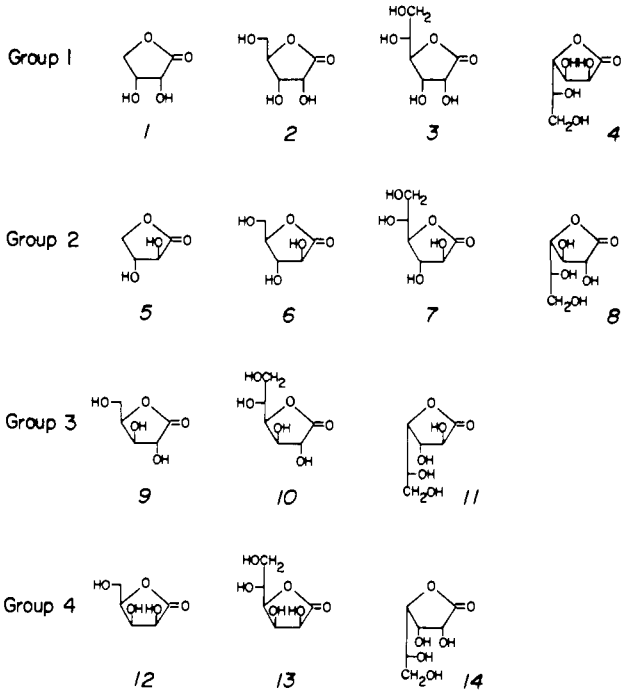

Results and Discussion

A. Structural Relationships in the D-Aldono-1,4-lactones. The simple D-aldono-1,4-lactone series comprises 14 compounds that can be organized into four structural groups based on similar ring configuration (Chart I). This organization will facilitate comparisons of NMR parameters and preferred ring conformation of configurationally related structures.

Group 1 contains compounds with *cis*-O2,O3 and *trans*-O3,C5 substituents, and includes the erythrono **1**, ribono **2**, allono **3**, and talono **4** configurations. Group 2 contains compounds with *trans*-O2,O3 and *trans*-O3,C5 substituents, and includes the threono **5**, arabinono **6**, altrono **7**, and galactono **8** configurations. Group 3 contains the xylono **9**, glucono **10**, and idono **11** configurations with *trans*-O2,O3 and *cis*-O3,C5 substituents, and group 4 contains the lyxono **12**, mannono **13**, and gulono **14** configurations with *cis*-O2,O3 and *cis*-O3,C5 substituents. Because C4 is prochiral in **1** and **5**, these compounds are also structurally related to those found in groups 4 and 3, respectively.

The formulation of structural groups in Chart I is based solely on the relative configuration of ring substituents. Configuration at C5 of hexono-1,4-lactones is not considered here, although it will certainly affect the conformation of the two-carbon exocyclic fragment in these compounds. It is not, however, an important determinant of ring conformation (see below) which is the focus of this study.

B. Assignment of ^{1}H and ^{13}C Chemical Shifts. Systematic studies of aldono-1,4-lactone conformations have been conducted by Horton and Walaszek[17,18] in which ^{1}H and ^{13}C NMR spectra were obtained for **2**, **6**, **8**, **9**, **10**, **12**, **13**, and **14**. ^{1}H spectra were obtained *in nonaqueous solvents* to simplify their interpretation at 100 MHz. ^{1}H Chemical shifts, ^{1}H–^{1}H couplings, and their conformational interpretation have not been obtained previously in the more biologically important water (^2H_2O) solvent. ^{13}C Chemical shifts in ^2H_2O were reported by Horton and Walaszek,[17,18] but their assignments remained tentative, as indicated in

(7) Perlin, A. S. *Methods Carbohydr. Chem.* **1962**, *1*, 64.
(8) Ball, D. H. *J. Org. Chem.* **1966**, *31*, 220.
(9) Morris, G. A.; Hall, L. D. *J. Am. Chem. Soc.* **1981**, *103*, 4703.
(10) Kiliani, H. *Ber. Dtsch. Chem. Ges.* **1885**, *18*, 3066.
(11) Serianni, A. S.; Nunez, H.; Barker, R. *J. Org. Chem.* **1980**, *45*, 3329.
(12) Schaffer, R.; Isbell, H. S. *Methods Carbohydr. Chem.* **1963**, *2*, 11.
(13) Frisell, W. R.; MacKenzie, C. G. *Methods Biochem. Anal.* **1958**, *6*, 63.
(14) Serianni, A. S.; Nunez, H. A.; Hayes, M. L.; Barker, R. *Methods Enzymol.* **1982**, *89*, 64.
(15) Serianni, A. S.; Barker, R. "Synthetic Approaches to Carbohydrates Enriched with Stable Isotopes of Carbon, Hydrogen and Oxygen", In *Isotopes in the Physical and Biomedical Sciences*; Jones, J., Buncel, E., Eds.; Elsevier: New York, 1987.
(16) (a) Hehre, W. J.; Stewart, R. F.; Pople, J. A. *J. Chem. Phys.* **1969**, *51*, 2657. (b) Binkley, J. S.; Whiteside, R. A.; Krishnan, A.; Seeger, R.; DeFrees, D. J.; Schlegel, H. B.; Topiol, S.; Khan, L. R.; Pople, J. A. *QCPE* **1981**, *13*, 406.
(17) Horton, D.; Walaszek, Z. *Carbonhydr. Res.* **1982**, *105*, 111.
(18) Walaszek, Z.; Horton, D. *Carbohydr. Res.* **1982**, *105*, 131.

Table II. ^1H Chemical Shifts for Aldono-1,4-lactones in ^2H_2O

compound	chemical shift (ppm)[a]							
	H2	H3	H4	H4′	H5	H5′	H6	H6′
erythro **1**	4.70	4.57	4.51	4.36				
ribo **2**	4.73	4.57	4.43		3.87	3.79		
allo **3**	4.78	4.56	4.53		3.95		3.76	3.69
talo **4**	4.76	4.47	4.58		3.97		3.67	3.61
arabino **6**	4.60	4.24	4.32		3.96	3.75		
altro **7**	4.60	4.40	4.33		4.10		3.75	3.64
galacto **8**	4.63	4.38	4.34		3.93		3.74	3.72
lyxo **12**	4.73	4.55	4.61		3.93	3.88		
manno **13**	4.74	4.60	4.44		4.00		3.83	3.70
gulo **14**	4.73	4.54	4.50		4.06		3.80	3.68

[a] Values are reported in ppm, are relative to sodium 3-(trimethylsilyl)-1-propanesulfonate (external), and are accurate to ±0.01 ppm. The more shielded C4 (**1**) and C5 (**2**, **6**, **12**) protons are designated as H4′ and H5′, respectively.

Table III. ^1H–^1H Coupling Constants[a] for Aldono-1,4-lactones in ^2H_2O

compound	coupled nuclei										
	2,3	3,4	3,4′	4,4′	4,5	4,5′	5,5′	5,6	5,6′	6,6′	2,4
erythro **1**	4.8	3.0	0.0	10.7							
ribo **2**	5.6	~0.6			3.3	4.0	13.0				
allo **3**	5.6	0			5.2			4.3	6.2	12.0	
talo **4**	5.7	0.7			2.4			5.8	7.2	11.6	0.4
arabino **6**	8.9	~8.8			2.2	4.5	13.3				
altro **7**	8.5	8.2			3.3			4.2	7.0	11.9	
galacto **8**	8.9	8.6			2.8			5.6	7.0	11.7	
lyxo **12**	4.8	2.9			4.6	7.1	12.6				
manno **13**	4.7	2.8			9.3			2.7	5.1	12.3	
gulo **14**	4.5	2.8			8.2			3.4	5.6	12.1	

[a] Values are reported in Hz and are accurate to ±0.1 Hz.

Table IV. ^{13}C–^1H Coupling Constants[a] for Aldono-1,4-lactones in ^2H_2O

compound	coupled nuclei			
	C1,H2	C1,H3	C1,H4	C1,H4′
erythro **1**	~4.6	8.3	~0.4	4.6
ribo **2**	~5.1	8.3	~3.7	
allo **3**	~5.2	8.3	3.9	
talo **4**	4.8	8.3	3.7	
arabino **6**	5.5	0	0.5	
altro **7**	5.5	0	0	
lyxo **12**	~4.8	8.6	~0.3	
manno **13**	~4.8	8.8	0	

[a] Values are reported in Hz and are accurate to ±0.1 Hz.

a recent review of ^{13}C chemical shifts of carbohydrates.[19]

^1H NMR spectra at 300 MHz were obtained in ^2H_2O for several aldono-1,4-lactones, and chemical shift assignments are given in Table II. Spectra were essentially first order (Figure 1A) and signal assignments were made based on internally consistent ^1H–^1H coupling patterns (Table III). The spectrum of **8**, however, was complex,[20] exhibiting virtual coupling at H2 and considerable signal overlap (Figure 2B); at 600 MHz these complications were eliminated (Figure 2A).

In **1**, **2**, **6**, and **12**, the more shielded prochiral C4 or C5 protons are designated as H4′ or H5′, respectively (Table II). A tentative stereochemical assignment of the C4 protons (H4, H4′) of **1** (Figure 1A) might be made by comparing chemical shifts in compounds **1**–**4** (group 1). The C4 protons of **2**, **3**, and **4** are cis to O3 and resonate between 4.43 and 4.58 ppm (av = 4.51 ppm), suggesting that the C4 proton of **1** resonating at 4.51 ppm (Table II) is cis to O3 and is, therefore, the pro-*S* proton. However, this assignment is incorrect for the following reasons. In **1**, $^3J_{H3,H4}$ = 3.0 Hz and $^3J_{H3,H4'}$ = 0 Hz (Table III). The latter coupling implies a dihedral angle between H3 and H4′ ($\theta_{H3,H4'}$) of ~90°, which can be attained only for the C4 proton cis to O3 regardless of ring conformation. When $\theta_{H3,H4'}$ is near orthogonal, $\theta_{C1,H4'}$ and $\theta_{C1,H4}$ are ~145 and ~100°, respectively, consistent with $^3J_{C1,H4'}$ = 4.6 Hz and $^3J_{C1,H4}$ = 0.4 (Table IV). Also, $^3J_{H3,H4}$ values in **2**, **3**, and **4** are small like $^3J_{H3,H4'}$ in **1**, as expected if H4′ is cis to O3 in **1** and ring conformation is conserved in group 1 (as concluded below); a comparison of $^3J_{C1,H4}$ in **2**, **3**, and **4** and $^3J_{C1,H4'}$

Table V. ^{13}C Chemical Shifts for Aldono-1,4-lactones in ^2H_2O

compound	chemical shift (ppm)[a]					
	C1	C2	C3	C4	C5	C6
erythro **1**	180.2	71.3	70.5	74.6		
ribo **2**	180.0	70.6	71.1	88.3	62.2	
allo **3**	179.7	70.3	69.7	87.6	71.7	63.5
talo **4**	180.0	70.2	71.8	87.7	72.1	63.4
threo **5**	178.8	74.6	73.7	71.1		
arabino **6**	177.6	75.2	73.8	82.6	60.7	
altro **7**	177.5	75.6	74.1	82.0	71.9	63.0
galacto **8**	177.5	75.3	74.5	81.6	70.5	63.6
xylo **9**	178.8	73.9	74.7	82.1	60.7	
lyxo **12**	179.6	71.9	71.0	83.0	61.2	
manno **13**	179.5	72.3	71.0	80.1	69.2	64.2
gulo **14**	179.5	72.4	71.2	82.9	71.7	63.1

[a] Chemical shifts are reported in ppm, are referenced (external) to the anomeric carbon of β-D-glucopyranose (97.4 ppm), and are accurate to ±0.1 ppm.

Table VI. ^{13}C–^{13}C Coupling Constants[a] for Aldono-1,4-lactones in ^2H_2O

compound	coupled nuclei			
	C1,C2	C1,C3	C1,C4	C1,C5
erythro **1**	56.2	2.5	2.1	
ribo **2**	55.7	2.8	2.2	0.0
allo **3**	55.8	2.8	2.2	0.0
talo **4**	55.9	2.9	2.3	0.0
threo **5**	55.9	8.0	0.0	
arabino **6**	55.7	7.7	0.0	1.7
altro **7**	55.7	7.7	0.0	1.5
galacto **8**	55.7	7.7	0.0	1.5
xylo **9**	56.0	7.8	0.7	0.0
lyxo **12**	55.8	1.8	2.0	1.7
manno **13**	55.9	1.6	1.8	1.9

[a] Values are reported in Hz and are accurate to ±0.1 Hz.

(19) Bock, K.; Pedersen, C. *Adv. Carbohydr. Chem. Biochem.* **1983**, *41*, 27.

(20) Walaszek and Horton[18] also observed these higher order effects in the 100-MHz ^1H NMR spctrum of **8** in [$^2H_5$]pyridine.

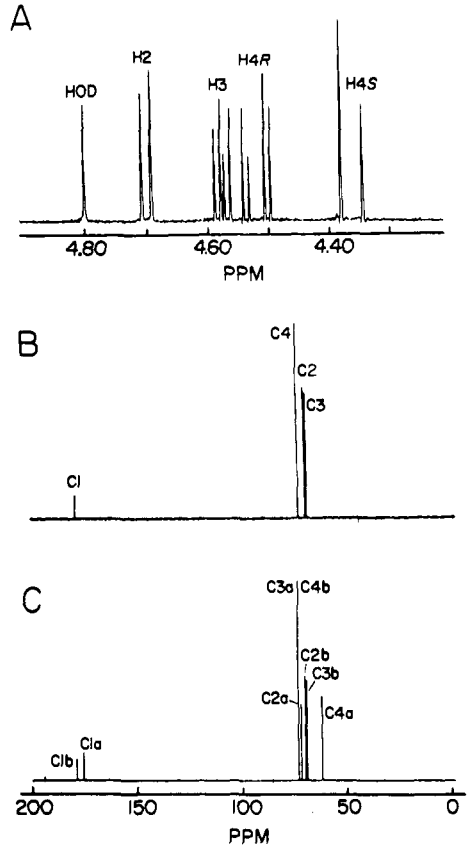

Figure 1. (A) The 300-MHz ^{1}H NMR spectrum of D-erythrono-1,4-lactone **1**, showing signal assignments. The stereochemical assignments of the C4 protons (H4*R*, H4*S*) are based on interpretation of $^3J_{HH}$ and $^3J_{CH}$ values (see text). Note that H3 appears as a quartet, being coupled only to H2 and H4*R* (not to H4*S*). This is verified from the splittings of H4*R* and H4*S* (quartet and doublet, respectively). (B) The ^{1}H-decoupled ^{13}C NMR spectrum (75 MHz) of a freshly prepared solution of **1** in ^2H_2O, showing signal assignments. (C) The ^{1}H-decoupled ^{13}C NMR spectrum (75 MHz) of the same solution in (B) after ~7 days of equilibration at ~25 °C, showing the presence of comparable amounts of free acid (a) and lactone (b). The chemical shifts (in ppm) of the free acid are: C1, 177.0; C2, 73.3; C3, 74.6; C4, 63.3.

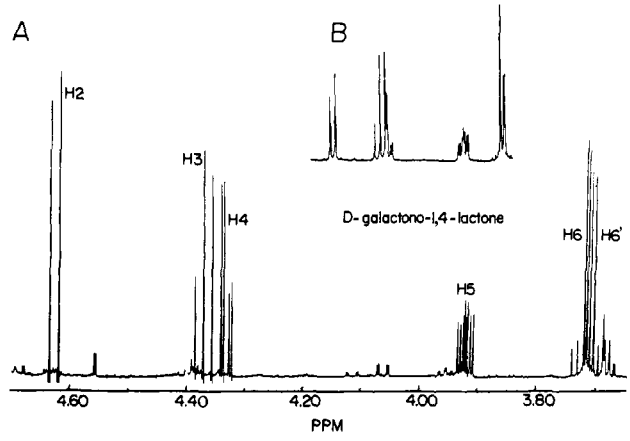

Figure 2. (A) The 600-MHz ^{1}H NMR spectrum of D-galactono-1,4-lactone **8** in ^2H_2O, showing signal assignments. This spectrum is essentially first order and was used to obtain J_{HH} values (Table III). (B) The 300-MHz ^{1}H NMR spectrum of **8** in ^2H_2O, showing considerable non-first-order behavior. For example, H2 appears as an apparent quartet caused by virtual coupling to H4. This spectrum cannot be interpreted without the aid of spectral simulation.

in **1** leads to the same conclusion. Therefore, from $^3J_{HH}$ and $^3J_{CH}$ correlations, the more shielded C4 proton of **1** (4.36 ppm) is the pro-*S* proton, a conclusion consistent with observations made earlier in the tetrofuranoses in which the more shielded C4 protons

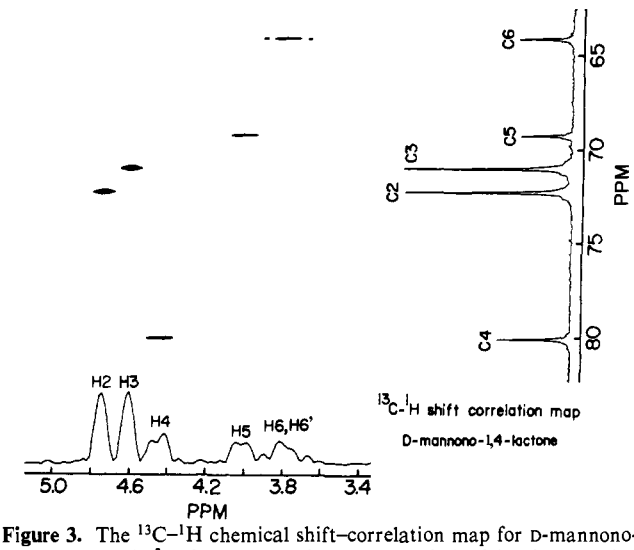

Figure 3. The ^{13}C–^{1}H chemical shift–correlation map for D-mannono-1,4-lactone **13** in ^2H_2O. The experiment was optimized for the detection of directly bonded protons. The low-resolution ^{1}H spectrum, obtained by projection, was sufficient to permit the assignment of carbons via cross-peaks, as shown. Similar spectra were obtained on the pentono- and remaining hexono-1,4-lactones, from which carbon assignments were made (Table V).

were found to be the pro-*S* protons.[3,21a] It is clear that stereochemical assignments of endocyclic methylene protons made solely by "chemical shift analogy" are not reliable. The assignments of the exocyclic hydroxymethyl protons in pentono-1,4-lactones **2**, **6**, and **12** are considered below in a discussion of C4–C5 bond conformation.

Firm assignments of ^{13}C chemical shifts (Table V) were made by 2D ^{13}C–^{1}H shift correlation spectroscopy (Figure 3) using the ^{1}H assignments in Table II. C2 assignments were confirmed from the ^{13}C spectra of [1-^{13}C]-enriched compounds by observation of $^1J_{C1,C2}$ (Table VI). The previously reported assignments for **1**[19] were found to be incorrect, while those for **5** have been confirmed. Again[22] we caution against making ^{13}C assignments based solely on structural analogies; the downfield to upfield sequence of δ_{C2}, δ_{C3}, and δ_{C4} for **5** differs completely from the δ_{C4}, δ_{C2}, and δ_{C3} pattern for **1** (Figure 1B).

C. ^{1}H–^{1}H, ^{13}C–^{1}H, and ^{13}C–^{13}C Coupling Constants. ^{1}H–^{1}H, ^{13}C–^{1}H, and ^{13}C–^{13}C couplings for several aldono-1,4-lactones are listed in Tables III, IV, and VI, respectively. These data reveal similarities in corresponding couplings *within* each configurational group and distinct differences in couplings *between* groups (Chart I). Two couplings, $^1J_{C1,C2}$ and $^2J_{C1,H2}$, are relatively insensitive to ring configuration. $^1J_{C1,C2}$ in 1,4-lactones (~56 Hz)[11] is ~11 Hz larger than in furanose rings (~45 Hz),[3,22-24] as expected from the increased s character of the C1–C2 bond in the former.[25] The insensitivity of $^2J_{C1,H2}$ (5.0 ± 0.3 Hz) to ring configuration implies that C2–H2 bond orientation is conserved in aldono-1,4-lactones; a preferred quasi-axial orientation is shown below.

D. Conformational Interpretation of Homo- and Heteronuclear Vicinal Couplings. In this discussion vicinal couplings (^{1}H–^{1}H, ^{13}C–^{1}H, ^{13}C–^{13}C) are interpreted in terms of preferred lactone ring and exocyclic group conformation.[26] The interpretation of

(21) (a) Wu, G. D.; Serianni, A. S.; Barker, R. *J. Org. Chem.* **1983**, *48*, 1750. (b) Kline, P. C.; Serianni, A. S., unpublished results.
(22) Snyder, J. R.; Serianni, A. S. *J. Org. Chem.* **1986**, *51*, 2694.
(23) Serianni, A. S.; Clark, E. L.; Barker, R. *Carbohydr. Res.* **1979**, *72*, 79.
(24) Snyder, J. R.; Serianni, A. S. *Carbohydr. Res.*, in press.
(25) Frei, K.; Bernstein, H. J. *J. Chem. Phys.* **1963**, *38*, 1216.
(26) The interpretation of $^3J_{HH}$ is based on a modified "Karplus"[27] curve described by Altona and co-workers (Haasnoot, C. A. G.; de Leeuw, F. A. A. M.; deLeeuw, H. P. M.; Altona, C. *Org. Magn. Reson.* **1981**, *15*, 43). "Karplus" curves for $^3J_{COCC}$, $^3J_{CCCH}$, and $^3J_{COCH}$ for coupling pathways characterized by a terminal carbonyl carbon have not been fully described; in this analysis, we assume that the shapes of these curves are similar to those determined for pathways in which all carbon atoms are sp^3-hybridized,[3,28] although their amplitudes are probably larger.

Scheme I

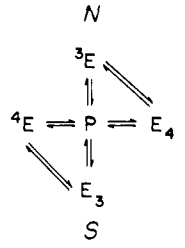

intra-ring $^{13}C-^{13}C$ couplings is complicated by the "dual-pathway" problem[29] and is discussed later.

The above-noted similarities in ^3J within each configurational group (Chart I) suggests that ring conformation (and possibly dynamics) is conserved within each group. Stated differently, lactone ring conformation is determined primarily by ring configuration, and is not noticeably affected by exocyclic structure and configuration.

Before examining these couplings, a model for lactone ring conformational dynamics should be considered. Because of the structural constraints imposed by the planar OC(O)C group, 1,4-lactone rings can assume only four envelope forms (E_3, ^3E, E_4, ^4E)[30] and the planar (P) form. Following the pseudorotational model for furanoses,[3,4] the interconversion between ^3E and E_4 conformers occurs via endocyclic bond rotations (Scheme I) and *does not require P as an intermediate*; the same is true for E_3-^4E interconversion (Scheme I). However, $^3E-E_3$, $^4E-E_4$, $^3E-^4E$, and E_3-E_4 interconversions do require P as an intermediate; unlike furanose rings, interconversion of "north" (N) and "south" (S)

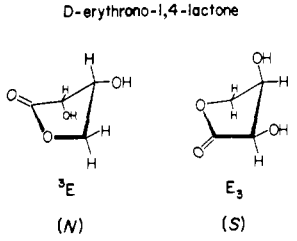

lactone ring conformers *must occur* by ring inversion. There is some suggestion[17,18] that ^4E and E_4 are less stable than ^3E and E_3 and that $^3E-E_3$ interconversion adequately describes lactone ring dynamics.

Discrimination by NMR (via spin couplings) between N and S conformers (e.g., ^3E and E_3) should be feasible. On the other hand, because of comparatively subtle differences in structure, discrimination between N (or S) conformers (e.g., ^3E and E_4) is not possible and other approaches (e.g., theoretical calculations) are required.

Group 1. The large $^3J_{C1,H3}$ (8.3 Hz) (Figure 4) in this group indicates that $\theta_{C1,H3} > 140°$, as found in *S* conformers. Further evidence is provided by $^3J_{H2,H3}$ and $^3J_{H3,H4}$; in *S* conformers, $\theta_{H2,H3}$ and $\theta_{H3,H4}$ are ~30 and ~90°, respectively, and couplings of 4.8–5.7 and 0–0.7 Hz, respectively, are consistent with these dihedral angles. In addition, in **2**, **3**, and **4**, $^3J_{C1,C5} = 0$ Hz and $^3J_{C1,H4} = 3.7–4.6$ Hz, as expected for *S* conformers where $\theta_{C1,C5} \simeq 110°$ and $\theta_{C1,H4} \simeq 130°$.

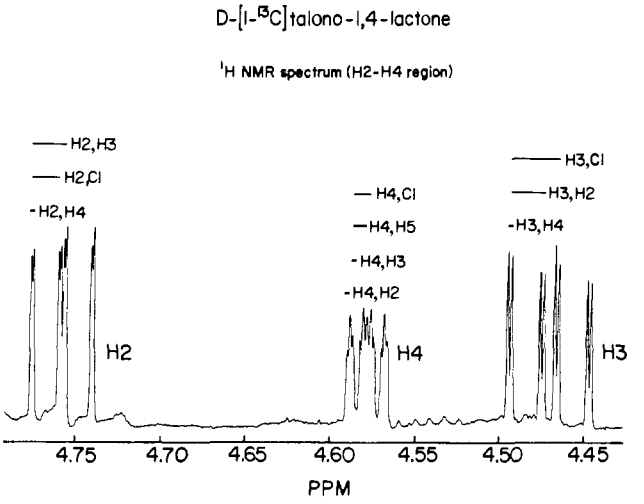

Figure 4. A portion of the 300-MHz ^1H NMR spectrum of D-[1-^{13}C]-talono-1,4-lactone 4, showing signals from H2, H3, and H4. By comparison to the spectrum of unenriched **4**, these multiplets can be resolved into $^1H-^1H$ and $^{13}C-^1H$ spin-coupling components; all three protons are coupled to C1, as shown (Table 1V). In addition to the expected $^3J_{HH}$ interactions, a four-bond coupling ($^4J_{HH}$) of 0.4 Hz occurs between H2 and H4.

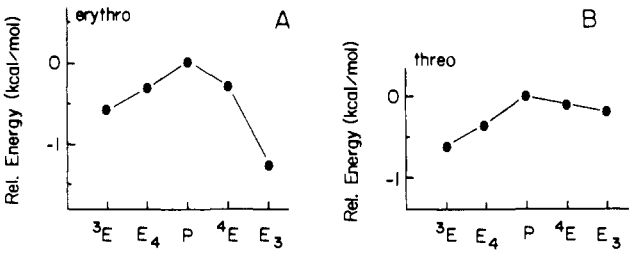

Figure 5. Plots of relative energy (kcal/mol) vs. ring conformation for D-erythrono-1,4-lactone **1** (A) and D-threono-1,4-lactone **5** (B). Energies were obtained from geometric optimization of each structure using Gaussian 80 (see Appendix for details).

Group 2. $^3J_{C1,H3}$ and $^3J_{C1,H4}$ values of ~0 Hz (Table IV) are consistent with N conformers in which $\theta_{C1,H3}$ and $\theta_{C1,H4} \simeq 90°$. Large values of $^3J_{H2,H3}$ and $^3J_{H3,H4}$ (~8.5 Hz) suggest $\theta_{H2,H3} \simeq \theta_{H3,H4} \simeq 160°$. The dihedral angle between C1 and C5 is ~130° in N conformers, which correlates with the observed 1.6 Hz coupling between these carbons.

Group 4. The large $^3J_{C1,H3}$ (~8.7 Hz) and small $^3J_{C1,H4}$ (~0.2 Hz) values (Table IV) are consistent with N conformers and are supported by $^3J_{H2,H3}$ (~4.6 Hz) ($\theta_{H2,H3} \simeq 40°$) and $^3J_{H3,H4}$ (2.8 Hz) ($\theta_{H3,H4} \simeq 40°$). In group 4, $^{13}C-^1H$ couplings are *required* for conformational analysis since $^1H-^1H$ couplings cannot be used alone to distinguish N and S conformers (i.e., $^1H-^1H$ couplings are expected to be similar in N and S conformers). As in group 2, the observed C1–C5 coupling (1.8 Hz) supports the preference for N conformers.

In summary, the coupling data indicate that aldono-1,4-lactones in aqueous solution *prefer conformations in which O2 orients quasi-equatorial, as observed previously*[17,18] *in nonaqueous solvents.*

E. Ab Initio Molecular Orbital Calculations. As discussed above, NMR spin couplings can discriminate between N and S lactone conformers but not between forms in each group (e.g., ^3E from E_4). This problem was addressed by conducting ab initio molecular orbital (MO) calculations at the STO-3G level on **1** and **5** which represent groups 1(4) and 2(3), respectively. The relative energies of the five "gas-phase" conformers (E_3, ^3E, E_4, ^4E, P) of each structure were determined through geometrical optimization. Optimized molecular parameters (bond lengths, angles, torsions) are listed in Tables VIII and IX of the Appendix.

These computations show that **1** and **5** prefer S and N conformers, respectively (Figure 5A,B). In **1**, E_3 is most stable, with

(27) Karplus, M. *J. Chem. Phys.* **1959**, *30*, 11.

(28) (a) For $^3J_{COCC}$: Walker, T. E.; London, R. E.; Whaley, T. W.; Barker, R.; Matwiyoff, N. A. *J. Am. Chem. Soc.* **1976**, *98*, 5807. (b) For $^3J_{CCCH}$: Schwarcz, J. A.; Perlin, A. S. *Can. J. Chem.* **1972**, *50*, 3667. (c) For $^3J_{COCH}$: Perlin, A. S.; Hamer, G. K. *Carbon-13 NMR in Polymer Science*; Pasika, W. M., Ed.; American Chemical Society: Washington, DC, 1979; p 123.

(29) (a) Marshall, J. L.; Faehl, L. G.; Kattner, R. *Org. Magn. Reson.* **1979**, *12*, 163. (b) Marshall, J. L. *Carbon–Carbon and Carbon–Proton NMR Couplings*; Verlag Chemie: Deerfield Beach, FL, 1983; pp 186–193.

(30) To simplify the discussion, only envelope forms will be considered, with the realization that intermediate twist conformers (e.g., $^3T_4$, $^4T_3$) are also possible.

the remaining conformers, including ^{4}E, having higher and comparable energies. By comparison, in **5**, ^{3}E appears most stable but is not much different in energy than the other conformers. In both **1** and **5**, the planar conformer is least stable. Qualitatively, these results agree with those obtained from solution studies by NMR.

It has been argued[17,18] that the preference for O2 of aldono-1,4-lactones to orient quasi-equatorial is caused by intramolecular hydrogen bonding between OH-2 and the carbonyl oxygen that is not possible (or is weaker) when O2 is quasi-axial. In our MO calculations, the initial C2–O2 torsions were chosen by model inspection to *minimize* this intramolecular hydrogen-bonding (see Appendix). In **1**, the distance between the carbonyl oxygen and the hydroxyl proton on O2 varies between 2.60 and 2.99 Å for the five optimized structures, the shortest distance occurring in E_3. Rotation of the C2–O2 bond increases this distance and prevents H-bonding to O1, but doing so could produce potential H-bonding interactions between the C2 and C3 hydroxyl groups that could complicate the calculations. However, in E_3, the C1—O1--H bond angle is ~73°, much smaller than the 120° considered optimal for H-bonding (this angular requirement is not rigid, but the great majority lie in the range 120 ± 15°).[31]

In **5**, calculations were conducted on structures in which the carbonyl oxygen–O2 hydrogen distances varied between 3.84 and 3.94 Å, and the optimized geometries forbid H-bonding to O1. In the absence of hydrogen bonding, therefore, these calculations show that conformers of **1** and **5** in which O2 is quasi-equatorial are still preferred, and suggest that other structural factors play a role in determining lactone ring conformation.

Riggs[32] has found from ab initio studies that the preferred conformation of 3-hydroxybutyrolactone orients O3 quasi-axial. The importance of this O3 orientation in aldono-1,4-lactones appears minor; for example, **9** and **12** orient O3 quasi-equatorial and quasi-axial, respectively, in order to accommodate a quasi-equatorial O2.

These results suggest that additional factors, perhaps stereoelectronic, govern O2 orientation in α-hydroxy-γ-lactone rings. The influence of nonbonding electrons on molecular structure and reactivity is well-recognized, important examples being the "anomeric effect",[31] "exoanomeric effect",[31] and "gauche effect".[31,33a,b] Molecular orbital calculations on **1** and **5** (see Appendix) reveal several notable structural trends that appear to depend on the disposition of oxygen lone-pair orbitals in these molecules. For example, in **1**, the C2–O2 and C2–H2 bonds decrease and increase in length, respectively, as the molecule converts from $^3E \rightarrow E_4 \rightarrow P \rightarrow {}^4E \rightarrow E_3$ (Table VIII of the Appendix). In E_3, the most stable conformer of **1**, the dihedral angle for the O1–C1–C2–O2 fragment is minimized (~40°), a geometry that could be stabilized by partial double-bond character of the C1–C2 and C2–O2 bonds. A similar trend is observed in **5**, in which the C2–O2 and C2–H2 bonds decrease and increase, respectively, in the direction $E_3 \rightarrow {}^4E \rightarrow P \rightarrow E_4 \rightarrow {}^3E$ (Table IX of the Appendix), as expected since ^{3}E is the most stable conformer of **5**. A comparison of the Mulliken populations for E_3 and ^{3}E conformers of **1** reveals that the C1–C2 and C2–O2 bonds have significantly greater π character in the former.[33c] This partial π-bond character in the ring atoms may be an important determinant of α-hydroxy-γ-lactone conformation in general.

C4–H4 bond lengths in **1** and **5** also appear to depend on conformation. Specifically, C4–H4*R* and C4–H4*S* bond lengths increase and decrease, respectively, as the rings convert from $^3E \rightarrow E_4 \rightarrow P \rightarrow {}^4E \rightarrow E_3$. It appears that C4–H4 bonds are longest when antiperiplanar (or nearly so) to a lone-pair orbital on the ring oxygen. This effect appears to be related to the observation[34a] that axial C2–H2 bonds of substituted 1,3-dioxanes undergo homolytic bond cleavage more readily than equatorial bonds because of favorable stereoelectronic interactions between the axial bond and adjacent antiperiplanar lone-pair orbitals on oxygen.

Table VII. Rotamer Distributions[a] about the C4–C5 Bond in Pentono-1,4-lactones Determined from ^{1}H–^{1}H Couplings in Table III

compound	P_{gg}	P_{gt}	P_{tg}
ribo **2**	0.64 (0.55)	0.19 (0.26)	0.17 (0.19)
arabino **6**	0.66 (0.61)	0.29 (0.32)	0.05 (0.07)
lyxo **12**	0.29 (0.08)	0.46 (0.59)	0.25 (0.33)

[a] Values were calculated using equations described in ref 44; values in parentheses were computed using equations described in ref 21a. See ref 21a for a discussion/comparison of both calculational approaches. Calculations were performed on an HP-11C calculator using a program to solve linear equations.

Our calculations show that C–H bond lengths in the E_3 conformation of **1** decrease in the order C2–H2 > C3–H3 ≃ C4–H4*R* > C4–H4*S* (Table VIII of the Appendix). *To a first approximation*, C–H bond length may be a determinant of ^{1}H chemical shieldings, with protons becoming more deshielded as bond lengths increase. If so, H2 would be most deshielded and H4*S* most shielded; H3 and H4*R* would have intermediate shieldings. This prediction is supported experimentally (Figure 1A). MO calculations also reveal different relative C–H bond lengths in each conformation, and, therefore, different NMR patterns for **1** in E_3 and E_4 conformations might be predicted. The C–H bond length, then, may be a factor in addition to others (e.g., "syn-upfield" rule[34b]) that affects ^{1}H shieldings in five-membered rings. In general, bond lengths as well as bond angles and torsions in 1,4-lactones respond to changes in conformation that implicate stereoelectronic factors as responsible in part for stabilizing/destabilizing particular geometries.

Finally, the relative energies of "gas-phase" structures determined from MO calculations will probably differ from those of "solvated" structures. However, the agreement between NMR and MO data implies that conformational preference is determined *by intrinsic molecular structure* in the absence of solvation. Solvation of **5** may play a significant role in further stabilization of N over S conformers, but the energy differences between N conformers (^{3}E, E_4) may still be small enough to permit significant amounts of both forms in solution. In **1**, however, assuming the absence of disproportionate solvent stabilization, E_3 is more stable than ^{4}E, as suggested from crystal structures of 1,4-lactones.[35a,b]

F. Hydroxymethyl Group Conformation in Pentono-1,4-lactones. Hydroxymethyl group conformation in sugars and sugar derivatives has received considerable attention in recent years.[21,36] Three staggered conformations are possible (gg, gt, and tg). From theoretical calculations on 1,2-dimethoxyethane, Wolfe[33a,b] has found that the conformer which orients the oxygens gauche is more stable than that having the anti orientation. This preference cannot be accounted for by steric and electrostatic factors alone, and provides the basis for the "gauche effect". A recent systematic study of hydroxymethyl group conformation in methyl D-pentofuranosides[21a] shows that gt and gg predominate over tg conformers, as predicted by this stereoelectronic effect.

Horton and Walaszek[17] have studied hydroxymethyl conformation in **2**, **6**, **9**, and **12** in nonaqueous solvents, and found the gg conformer to predominate in all but **12**, where tg was reported to be preferred. Using $^3J_{H4,H5}$ and $^3J_{H4,H5'}$ values (Table III) and assuming by analogy to pentofuranosides[21a] and ribonucleosides[21b]

(31) Kirby, A. J. *The Anomeric Effect and Related Stereoelectronic Effects at Oxygen*; Springer-Verlag: New York, 1983.

(32) A recent ab initio study of butyrolactone and 3-hydroxybutyrolactone has shown that, in these systems, the 3-21G split-valence basis set yields results in closer agreement with crystallographic data than does the STO-3G basis set. See: Riggs, N. V. *Aust. J. Chem.* **1985**, *38*, 1575.

(33) (a) Wolfe, S. *Acc. Chem. Res.* **1972**, *5*, 102. (b) Zefirov, N. S.; Samoshin, V. V.; Subbotin, O. A.; Baranenkov, V. I.; Wolfe, S. *Tetrahedron* **1978**, *34*, 2953. (c) The STO-3G Mulliken π-overlap populations for **1** in the ^{3}E conformation are 0.006 electron for C1–C2 and 0.006 electron for C2–O2. In the more stable E_3 conformation, the same populations are 0.008 and 0.011 electron, respectively.

(34) (a) Beckwith, A. L. J.; Easton, C. J. *J. Am. Chem. Soc.* **1981**, *103*, 615. (b) Anteunis, M.; Danneels, D. *Org. Magn. Reson.* **1975**, *7*, 345.

(35) (a) Berman, H. M.; Rosenstein, R. D.; Southwick, *Acta Crystallogr., Ser. B* **1971**, *27*, 7. (b) Jeffrey, G. A.; Rosenstein, R.D.; Vlasse, M. *Acta Crystallogr.* **1967**, *22*, 725.

(36) (a) Ohrui, H.; Nishida, Y.; Watanabe, M.; Hori, H.; Meguro, H. *Tetrahedron Lett.* **1985**, *26*, 3251. (b) De Bruyn, A.; Anteunis, M. *Carbohydr. Res.* **1976**, *47*, 311.

Chart II

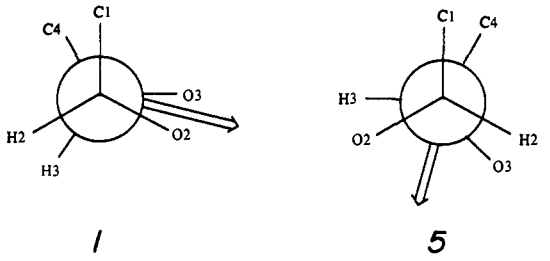

that the more shielded C5 proton is pro-*R* (this assumption is reasonable in light of these recent observations[21] but nevertheless requires validation by stereoselective deuteration[21]), C4–C5 bond rotamer distributions in ^2H_2O for **2**, **6**, and **12** were calculated and are given in Table VII. These results differ from those of Horton and Walaszek[17] for **12**, possibly because of error in their reported couplings or to hydroxymethyl conformation which is solvent dependent. In **2** and **6**, the gg conformer is preferred in which O4 and O5 are gauche. In **12**, however, this conformation is destablized by a 1,3-interaction between O3 and O5, causing the alternate rotamer having O4 and O5 gauche (gt) to be preferred, not the tg conformer (predicted to be least stable by the "gauche effect").

In pentono-1,4-lactones and methyl pentofuranosides[21a] in ^2H_2O, then, C4–C5 bond conformations are preferred in which O4 and O5 are gauche. As ring substituents cis to C5 are removed, gg increases in proportion, permitting O5 to orient "over" the ring. The different conformational preferences of 1,4-lactone rings probably affect hydroxymethyl group conformation just as ring conformation appears to be coupled to C4′–C5′ bond conformation in nucleosides.[37] In addition to the "gauche effect",[33a] steric effects, and ring conformation, solvation and the tendency to minimize the net molecular dipole moment may affect rotamer distribution. The relative strengths of these factors in carbohydrates remain to be assessed.

G. Intra-Ring ^{13}C–^{13}C Coupling in Aldono-1,4-lactones. The interpretation of intra-ring ^{13}C-^{13}C coupling constants in five-membered rings requires an assessment of the contributions that two "through-bond" pathways make to the observed values.[29a,b] For example, coupling between C1 and C3 (Table VI) in lactones occurs via two-bond (C1–C2–C3) and three-bond (C1–O4–C4–C3) pathways; the corresponding dual-pathway coupling constant is denoted as $^{2+3}J_{C1,C3}$. A similar situation is encountered with couplings between C1 and C4 (Table VI). Of course, it is possible that "through-space" mechanisms[38] may also modulate such interactions, but this contribution is probably small.

It has been proposed[29a] that $^{2+3}J_{CC}$ values are equal to the algebraic sum of the couplings for each component pathway, and, therefore, coupling signs for each pathway must be known to interpret them. These sign determinations are not straightforward.[39] Furthermore, ring conformation must be well-defined before "Karplus" and other empirical relationships can be applied to calculate the constituent two- and three-bond ^{13}C–^{13}C couplings.

The interpretation of intra-ring ^{13}C–^{13}C couplings in previous studies of furanose rings[3,22,24] was hindered in part by the presence of conformational heterogeneity. By comparison, aldono-1,4-lactones are more conformationally rigid and represent a better ring system to study.

An examination of data in Table VI reveals some noteworthy trends. Group 1 structures are characterized by $^{2+3}J_{C1,C3}$ = 2.8 Hz and $^{2+3}J_{C1,C4}$ = 2.2 Hz. In group 2, $^{2+3}J_{C1,C3}$ is significantly larger (7.8 Hz) and $^{2+3}J_{C1,C4}$ = 0 Hz. In group 4, $^{2+3}J_{C1,C3}$ = 1.7 Hz and $^{2+3}J_{C1,C4}$ = 1.9 Hz. Intra-ring ^{13}C–^{13}C couplings within groups 1(4) and within groups 2(3) are similar *despite significant differences in ring conformation.* Clearly, relative configuration of the ring substituents plays the key role here.

Some understanding of $^{2+3}J_{C1,C3}$ accrues from examining C1–C2–C3 geometry in **1** and **5** (Chart II). In **1** (E_3 conformer), O2 and O3 are oriented with their *net dipole moment approximately orthogonal* to the O1–C1–C2 bond fragment; this geometry is characteristic of group 1 and 4 structures. On the other hand, in **5** (^3E conformer), O2 and O3 are oriented with their *net dipole moment approximately antiperiplanar* to the same fragment; this geometry characterizes group 2 and 3 structures. In **1** and **5**, the three-bond contribution to $^{2+3}J_{C1,C3}$ should be similar if puckering amplitudes in these structures are comparable. Therefore, the significant difference in $^{2+3}J_{C1,C3}$ values must be due to the two-bond contribution, with O2–O3 orientation in **5** (Chart II) producing greater coupling. To generate the large observed coupling to C3 in **5**, coupling signs for both pathways are probably the same (both negative or both positive) but this remains to be verified experimentally.

The smaller and similar $^{2+3}J_{C1,C4}$ values in **1** and **5** can be rationalized from the above considerations. The two-bond coupling is probably small in both structures because of the lack of electronegative substituents oriented properly along this pathway to enhance coupling (Chart II); the heteroatom in the pathway may also modify this coupling. The small difference in $^{2+3}J_{C1,C4}$ between groups 1(4) (~2.1 Hz) and groups 2(3) (0 Hz) may be due primarily to the effect of substituent geometry on $^3J_{CCCC}$, again

Table VIII. Molecular Dimensions Obtained from STO-3G Optimization of Planar and Envelope Forms of D-Erythrono-1,4-lactone **1**

parameter[a]	^3E	E_4	P	^4E	E_3
R12	1.565	1.565	1.562	1.565	1.562
R23	1.553	1.557	1.557	1.558	1.553
R34	1.564	1.566	1.570	1.565	1.563
R45	1.439	1.438	1.437	1.438	1.441
R51	1.400	1.400	1.395	1.399	1.398
R16	1.212	1.212	1.213	1.212	1.212
R27	1.096	1.097	1.098	1.098	1.100
R28	1.435	1.434	1.433	1.432	1.429
R89	0.992	0.992	0.993	0.992	0.992
R310	1.097	1.097	1.096	1.096	1.096
R311	1.429	1.430	1.432	1.433	1.432
R1112	0.992	0.992	0.992	0.991	0.991
R413	1.094	1.093	1.095	1.096	1.096
R414	1.096	1.097	1.096	1.094	1.094
A123	101.8	103.1	104.0	103.4	102.2
A234		103.3	104.3	103.0	
A345	107.8	108.1	110.0	108.5	108.2
A451	109.1	108.4	110.1	108.3	108.7
A512	110.8	111.1	111.7	111.1	110.7
A516	121.5	121.8	121.6	121.9	122.2
A127	110.0	109.0	108.5	108.4	107.8
A128	111.5	111.9	112.1	112.7	113.5
A289	103.7	103.4	103.4	103.4	103.4
A4310	109.1	109.1	109.5	110.0	110.4
A4311	114.2	113.7	113.0	112.9	112.8
A31112	103.8	103.8	103.7	103.8	104.0
A5413	108.4	108.4	108.7	109.8	109.8
A5414	110.1	110.1	108.9	108.5	108.6
T3451	17.9				18.4
T4512	0.0	15.2	0.0	15.1	0.0
T5123		0.0	0.0	0.0	
T4516	178.7	165.2	178.6	167.8	179.4
T5127	136.3	118.1	117.5	116.6	97.2
T5128	99.1	118.3	119.4	119.9	138.7
T7289	55.5	62.3	64.4	65.8	72.1
T54310	86.8	92.4	117.4	141.5	147.1
T54311	147.6	142.7	118.4	93.5	87.0
T1031112	56.8	55.7	54.8	56.1	55.4
T15413	139.8	146.3	122.0	96.4	102.1
T15414	101.5	95.1	120.3	145.4	139.6

[a] R denotes bond lengths in Å between the indicated atoms (structure i). A and T denote bond angles and torsions, respectively, in degrees.

(37) For a recent discussion of this observation in nucleosides (-tides) see: Saenger, W. *Principles of Nucleic Acid Structure*; Springer-Verlag: New York, 1984; pp 79–81.

(38) Marshall discusses this mechanism in ref 29b, pp 107–114.

(39) (a) Hansen, P. E.; Poulsen, O. K.; Berg. A. *Org. Magn. Reson.* **1975**, *7*, 405. (b) Linde, S. A.; Jakobsen, H. J. *J. Am. Chem. Soc.* **1976**, *98*, 1041. (c) Hansen, P. E.; Paulsen, O. K.; Berg, A. *Org. Magn. Reson.* **1976**, *8*, 632. (d) See ref 29b, pp 178–186.

Table IX. Molecular Dimensions Obtained from STO-3G Optimization of Planar and Envelope Forms of D-Threono-1,4-lactone **5**

parameter[a]	^{3}E	E_4	P	^{4}E	E_3
R12	1.560	1.561	1.560	1.562	1.561
R23	1.555	1.558	1.558	1.559	1.557
R34	1.563	1.564	1.567	1.563	1.562
R45	1.438	1.437	1.436	1.437	1.438
R51	1.403	1.403	1.399	1.402	1.401
R16	1.210	1.211	1.211	1.211	1.211
R27	1.099	1.098	1.098	1.097	1.096
R28	1.430	1.432	1.433	1.433	1.434
R89	0.991	0.991	0.991	0.991	0.991
R310	1.097	1.097	1.097	1.097	1.097
R311	1.430	1.431	1.432	1.433	1.432
R1112	0.991	0.991	0.991	0.991	0.991
R413	1.094	1.093	1.095	1.096	1.096
R414	1.097	1.097	1.096	1.094	1.095
A123	102.6	103.4	104.1	103.5	102.7
A234	103.2	104.4	103.4		
A345	108.3	108.2	109.8	108.6	108.6
A451	109.3	108.6	110.3	108.9	109.4
A512	110.7	110.8	111.4	110.9	110.9
A516	121.2	121.4	121.1	121.4	121.3
A127	108.5	108.8	108.7	108.9	109.6
A128	109.3	108.7	108.4	108.3	108.0
A289	103.7	103.8	103.9	104.0	104.0
A4310	109.7	109.6	109.7	109.9	110.1
A4311	114.0	113.7	113.4	113.6	113.6
A31112	104.4	104.4	104.4	104.5	104.4
A5413	108.6	108.4	108.8	109.9	109.6
A5414	110.0	110.2	109.0	108.5	108.7
T3451	16.0				15.1
T4512	0.0	15.1	0.0	13.6	0.0
T5123	0.0	0.0	0.0		
T4516	179.8	166.5	179.6	168.4	180.1
T5127	99.3	115.6	116.0	116.2	131.7
T5128	138.4	122.3	122.2	121.6	105.7
T7289	54.9	50.7	50.7	50.0	49.8
T54310	90.4	92.4	117.1	138.8	141.7
T54311	143.6	141.9	117.9	95.7	92.4
T1031112	55.9	55.6	57.6	60.4	61.0
T15413	138.2	146.3	121.8	98.6	105.2
T15414	103.4	95.2	120.5	143.2	136.6

[a] R denotes bond lengths between the indicated atoms (structure i) in Å. A and T denote bond angles and torsions, respectively, in degrees.

assuming that puckering amplitudes are similar. In simpler lactones, $^2J_{COC}$ and $^3J_{CCCC}$ involving the carbonyl carbon appear to have positive signs,[40] so that $^{2+3}J_{C1,C4}$ may have a net (+) sign.

The above arguments can be tested by comparing intra-ring ^{13}C–^{13}C coupling in 3-deoxy-D-[1-^{13}C]ribono- and arabinono-1,4-lactones. Removal of O3 in **6** is predicted to decrease $^{2+3}J_{C1,C3}$ significantly to a value similar to that found in **2**; removal of O3 in **2** should have little effect on $^{2+3}J_{C1,C3}$. C3 deoxygenation should have a minor effect on $^{2+3}J_{C1,C4}$ in **2** and **6**. Ultimately, coupling signs for each pathway (C1–O4–C4, C1–C2–C3, C1–O4–C4–C3, C1–C2–C3–C4) in 1,4-lactone rings must be established before a complete interpretation of $^{2+3}J_{CC}$ in this system is possible.

H. Tautomeric Composition of Aqueous Solutions of Aldono-1,4-lactones. Horton and Walaszek[17] have reported that equilibrated aqueous solutions of pentono-1,4-lactones contain both linear (free acid) and cyclic forms. The ^{13}C NMR of an equilibrated solution of the tetrono-1,4-lactone **1** in ^2H_2O (Figure 1C) also shows the presence of two forms.[41] It is interesting to note that the C4 signal of the free acid is ~10 ppm upfield from C4 of the lactone, as predicted from empirical rules.[19] This chemical shift difference should permit the application of 2D chemical exchange spectroscopy[42] and/or selective irradiation NMR methods[43] to measure the rates of interconversion between linear and cyclic forms. [^{13}C] enrichment at C4 would facilitate these studies. Also, the [1-^{13}C]-enriched lactones prepared for this study can be hydrolyzed to study the conformations of the free acids and their salts (aldonates). Studies such as these may shed further light on free acid–lactone interconversion in solution.

Summary

This investigation has utilized NMR and calculational (MO) methods to address several aspects of aldono-1,4-lactone chemistry. The results are summarized as follows.

(a) Chemical methods have been described for the preparation and purification of several D-[1-^{13}C]aldono-1,4-lactones.

(b) ^{1}H NMR spectra in ^2H_2O have been interpreted, and ^{13}C spectra have been assigned with the aid of 2D ^{13}C-^{1}H chemical shift correlation spectroscopy. Some ^{13}C resonances have been reassigned.

(c) Preferred conformations of aldono-1,4-lactones have been determined with the use of ^{1}H–^{1}H, ^{13}C–^{1}H, and ^{13}C–^{13}C coupling constants. In the compounds examined, conformations are preferred in which O2 orients quasi-equatorial. Ab initio MO calculations at the STO-3G level suggest that intramolecular hydrogen bonding is not the key factor in stabilizing preferred geometries, but increased π character of the C1–C2 and C2–O2 bonds may play a role. Stereoelectronic effects of oxygen lone-pair orbitals on C–H bond lengths in lactone rings are indicated by these calculations, and may play a role in determining ^{1}H chemical shieldings.

(d) Hydroxymethyl conformations in pentono-1,4-lactones have been examined. In aqueous solution, the preferred C4–C5 conformer is gg for ribo and arabino configurations, and gt for the lyxo configuration.

(e) The dual-pathway ^{13}C–^{13}C coupling problem in aldono-1,4-lactone rings has been addressed. An O2–O3 dipole model has been proposed to explain the dependence of C1–C3 coupling on relative configuration at C2 and C3.

Acknowledgment. This work was supported by the Research Corporation (10028), the National Institutes of Health (GM 33791), and Omicron Biochemicals Inc., Ithaca, New York. A.S. thanks Dr. Daniel Chipman of the Notre Dame Radiation Laboratory for help in conducting the MO calculations and for useful discussions, the Notre Dame Computing Center for access to the IBM 370/3033 mainframe computer, and Joseph R. Snyder for obtaining several 2D ^{13}C–^{1}H shift-correlated spectra. We also thank Dr. Mishra at Carnegie-Mellon University for obtaining the 600-MHz ^{1}H NMR spectrum of D-galactono-1,4-lactone, and Rosemary Patti for typing the manuscript.

Appendix: Ab Initio STO-3G Molecular Orbital Calculations of Preferred Geometries of D-Erythrono-1,4-lactone 1 and D-Threono-1,4-lactone 5.

A. Selection of Initial Molecular Parameters. Geometric optimization using Gaussian 80[16] requires the choice of initial estimates of bond lengths (R), angles (A), and torsions (T). The 14 atoms of lactones **1** and **5** were identified by number (structure i) to accommodate the required *Z*-matrix data entry format of

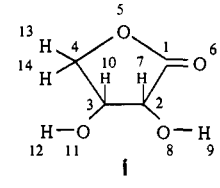

i

the program. Initial estimates of bond lengths and angles were based on similar parameters determined previously by crystallography on related structures.[35a,b] The choice of endocyclic torsions depended on the conformer being optimized; for example,

(40) See ref 29b, p 190.
(41) It is not clear at present whether the mixture in Figure 1C represents the true thermodynamic equilibrium.
(42) Huang, Y.; Macura, S.; Ernst, R. R. *J. Am. Chem. Soc.* **1981**, *103*, 5327.
(43) Serianni, A. S.; Pierce, J.; Huang, S.-G.; Barker, R. *J. Am. Chem. Soc.* **1982**, *104*, 4037.
(44) Manor, P. C.; Saenger, W.; Davies, D. B.; Jankowski, K.; Rabczenko, A. *Biochim. Biophys. Acta* **1974**, *340*, 472.

for ^3E, the torsions T4512 and T3451 were set to 0 and ~20°, respectively. T3451 determines the initial puckering amplitude of the ring. In each calculation, the 0° endocyclic torsion that constrains the analysis to a particular puckered form was held constant; the puckering angle, however, was optimized.

The initial exocyclic torsions T7289 and T1031112, which define the orientation of the 2-OH and 3-OH protons, were chosen by model inspection to minimize possible intramolcular hydrogen-bonding interactions. Thus, in **1**, C3–C2–O2–H and C2–C3–O3–H torsions were 180°, as were the C1–C2–O2–H and C2–C3–O3–H torsions in **5**. This approach is certainly not ideal and may affect results as discussed previously in molecular mechanics studies.[45] It is, however, impractical to conduct calculations for each C–O torsion; to do so requires nine optimizations for each conformer. This initial choice of C–O torsions should minimize the problem of differential stabilization of conformers by intramolecular H-bonding which, if present, could significantly affect energy profiles and lead to erroneous conclusions.

Five conformers (^3E, E_3, ^4E, E_4, P) of **1** and **5** were optimized with the STO-3G basis set, each calculation requiring approximately 5 h of CPU time (IBM 370/3033 mainframe) to reach convergence.

B. Optimized Molecular Parameters. The optimized molecular parameters determined for the five conformers of **1** and **5** are listed in Tables VIII and IX. The predicted bond lengths (R), angles (A), and torsions (T) are consistent with similar parameters well-established by crystallography (e.g. R_{CC} = 1.55 Å, R_{CO} = 1.43 Å, $R_{C=O}$ = 1.21 Å).

Several observations are noteworthy. The C4–O4 bond length (R45) is clearly longer (av 1.438 Å) than that between O4 and C1 (R51) (av 1.399 Å), indicating partial double-bond character of the latter. Crystallographic studies show a more pronounced difference (1.472 and 1.346 Å, respectively[35]). Use of a split-valence basis set (e.g., 3-21G*), which includes d-orbital contributions, may yield better agreement between calculation and experiment.[32]

Predicted endocyclic bond angles show a dependence on the type and sequence of atoms defining the angle, with COC > CCO > CCC, where the central atom in sp^3-hybridized. Similar observations have been made previously on furanoses by calculation[2a] and crystallography.[35] The sum of the endocyclic angles for planar forms (P) is 540°, as predicted for a pentagon, whereas in puckered forms this sum decreases by ~6°. In contrast to exocyclic angles (A289, A31112), endocyclic angles appear to be sensitive to ring conformation.

Of interest is the predicted puckering angle of the lactone ring. In both **1** and **5**, this angle appears to depend on ring conformation, varying between 14 and 18°. Cremer and Pople[1e] have shown that puckering amplitudes predicted using the STO-3G basis set are often small compared to those measured experimentally and that inclusion of polarization functions in the computation may improve the result. Based on their observations, it is unlikely, however, that these values are in error by more than 5–10°.

The results of these computations, especially the predicted total energies, should be viewed with some caution. As shown in Figure 5 of the text, the energy differences between "gas-phase" conformers are small (0–1.3 kcal/mol), and failure to consider all potential factors (e.g., polarization functions, d orbitals, C–O torsions) in these computations could lead to error. Additional factors in solution (e.g., solvent–solute interactions) will certainly affect relative stabilities. The calculations do predict the same most stable conformer of **1** and **5** in the "gas phase" as suggested in solution by NMR methods, showing that these preferences are determined by the intrinsic structure of the molecule (see text). However, the NMR data suggest greater energy differences between N and S conformers than theory predicts, and it is not clear whether further stabilization is offered by solvation effects (which may be simulated by Monte Carlo methods) or whether the current "gas-phase" computations do not predict these differences accurately.

Registry No. [1-^{13}C]-**1**, 108269-40-5; [1-^{13}C]-**2**, 108341-65-7; [1-^{13}C]-**3**, 108269-41-6; [1-^{13}C]-**4**, 108269-42-7; [1-^{13}C]-**5**, 108341-66-8; [1-^{13}C]-**6**, 108341-67-9; [1-^{13}C]-**7**, 78814-13-8; [1-^{13}C]-**8**, 108269-43-8; [1-^{13}C]-**9**, 108341-68-0; [1-^{13}C]-**10**, 108269-44-9; [1-^{13}C]-**12**, 108341-69-1; [1-^{13}C]-**13**, 40010-59-1; [1-^{13}C]-**14**, 108269-45-0; D-[1-^{13}C]-erythrose, 70849-19-3; D-[1-^{13}C]threose, 70849-20-6.

(45) (a) Lesyng, B. *Carbohydr. Res.* **1984**, *133*, 187. (b) Burkert, U.; Allinger, N. L. *Molecular Mechanics*; American Chemical Society: Washington, DC, 1982; pp 257–265.